Nanoscale

Accepted Manuscript

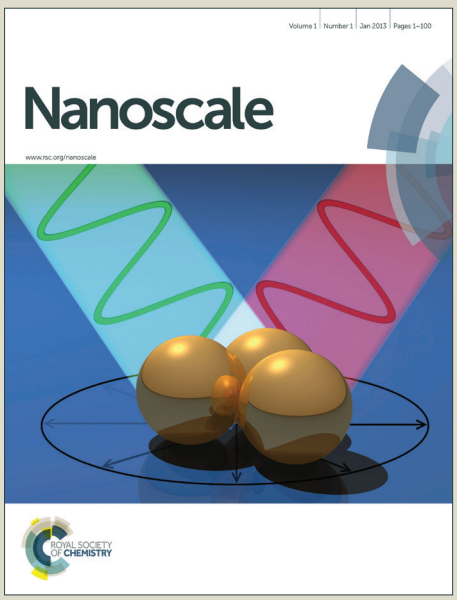

ROYAL SOCIETY OF CHEMISTRY

www.rsc.org/nanoscale

Modeling Nanoparticle Wrapping or Translocation in Bilayer Membranes

Emily M. Curtis[1], Amir H. Bahrami[1,2], Thomas R. Weikl[2], Carol K. Hall[1]

[1] Department of Chemical and Biomolecular Engineering, North Carolina State University, Engineering Building I, 911 Partners Way, Raleigh, North Carolina 27695-7905, United States

[2] Max Planck Institute of Colloids and Interfaces, Department of Theory and Bio-Systems, Science Park Golm, 14424 Potsdam, Germany

Table of Contents Entry

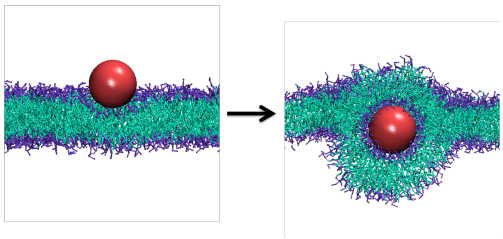

The molecular level interaction between nanoparticles and lipid membranes, including wrapping, is simulated using discontinuous molecular dynamics with the LIME force field.

Abstract

The spontaneous wrapping of nanoparticles by membranes is of increasing interest as nanoparticles become more prevalent in consumer products and hence more likely to enter the human body. We introduce a simulations-based tool that can be used to visualize the molecular level interaction between nanoparticles and bilayer membranes. By combining LIME, an intermediate resolution, implicit solvent model for phospholipids, with discontinuous molecular dynamics (DMD), we are able to simulate the wrapping or embedding of nanoparticles by 1,2-dipalmitoyl-*sn*-

glycero-3-phosphocholine (DPPC) bilayer membranes. Simulations of hydrophilic nanoparticles with diameters from 5Å to 100Å and different masses per volume. show that hydrophilic nanoparticles with diameters greater than 20Å become wrapped while those with diameters less than 20Å do not . Instead these smaller particles become embedded in the bilayer surface where they can interact with the hydrophilic head groups of the lipid molecules. Nanoparticle density does not play a significant role in the wrapping of hydrophilic nanoparticles. We also investigate the interaction between a DPPC bilayer and hydrophobic nanoparticles with diameters 5Å to 40Å. These nanoparticles do not undergo the wrapping process; instead they directly penetrate the membrane and embed themselves within the inner hydrophobic core of the bilayers. The density of hydrophobic nanoparticles does not appear to affect the way in which they interact with the membranes.

Introduction

In this work, we consider the interaction between nanoparticles and biomembranes and the attendant wrapping or penetration that follows from this interaction. Motivation for this study comes from the increasing prevalence of nanoparticles in our everyday lives, the use of nanoparticles to deliver drugs, proteins, and antimicrobials into cells, and concerns about nanoparticle toxicity. For a nanoparticle to be wrapped by, or penetrate through, a cell membrane, specific (ligand-receptor) and nonspecific (surface charge, hydrophobicity, size and shape) binding interactions must overcome the resistive forces associated with membrane stretching and elasticity.[1] Wrapping can be described as the process by which a

membrane bends its structure in order to maximize the number of interactions it has with a nanoparticle. During wrapping the lipid head groups of a membrane form a vesicle around the nanoparticle. This is different than embedding, the process by which a nanoparticle penetrates into a membrane with minimal disruption to the structure. Experimental studies have been performed to investigate the role that both specific and nonspecific interactions play in the cellular uptake of nanoparticles [1,2,3,4,5], however, the complexity and diversity of nanoparticle types that currently exist make it very difficult to completely explore the behavior of all nanoparticle/membrane systems. Computer simulation is a tool that could be used to aid this effort by allowing visualization of the molecular motions that contribute to both the wrapping and direct penetration processes that occur at nanoparticle/membrane interfaces.

Our goal has been to develop a computational model that provides molecular-level insights into, and facilitates the exploration of, the interaction between biomembranes and nanoparticles with different geometric and energetic properties. In this paper we demonstrate how the combination of discontinuous molecular dynamics simulations (DMD) and our previously-developed LIME forcefield [6] can be used to model the interaction between lipid membranes and nanoparticles of different sizes, densities and hydrophobicities. We show that LIME/DMD simulations can be used to study the wrapping of hydrophilic nanoparticles of size range 5-100 Å by a lipid membrane and the mechanism by which a hydrophobic nanoparticle penetrates the inner core of a bilayer.

A number of experimental studies have been conducted to examine the interaction between nanoparticles and bilayer membranes. Chithrani and co-workers investigated the intracellular uptake by mammalian HeLa cells of gold nanoparticles with different sizes and shapes.[3] Rod-shaped nanoparticles with dimensions of 40x14nm and 74x14nm and spherical nanoparticles with diameters of 14, 30, 50, 74 and 100 nm were studied. The cells were incubated with the gold nanoparticles for 6 hours. Subsequently, the concentration of Au that had accumulated in the cells was measured. The cellular uptake of spherical nanoparticles exhibited a maximum as a function of nanoparticle size; it was larger for particles with diameters of 30nm and 50nm and smaller for particles with diameters of 14nm, 74nm and 100nm. Cellular uptake for rod-shaped particles was lower than that for spherical particles.[3] The authors speculated that the difference in the uptake between the various sizes and shapes of nanoparticles could be due to surface curvature and the amount and type of proteins absorbed onto the nanoparticle surface.

Bihan and co-workers conducted experiments to study how the size of silica nanoparticles affects the engulfing process by DOPC liposomes.[7] According to their results, silica nanoparticles with diameters of 30, 65 and 190 nm were engulfed by the liposomes, while those with diameters of approximately 15-20 nm remained bound to the outer surface of the liposome. The authors explain that although the 15-20 nm nanoparticles interacted with the DOPC lipid membrane in the same way as the larger nanoparticles, the adhesive strength was not sufficient to

induce a curvature of the lipid membrane and to subsequently trigger the engulfing process.[7]

Win and co-workers investigated the effect of particle size and surface coating on the cellular uptake of polymeric nanoparticles intended for the oral delivery of anticancer drugs.[4]. The authors evaluated the cellular uptake of 50nm, 100nm, 200nm 500nm and 1000nm polystyrene nanoparticles by Caco-cells. The 100nm and 200nm nanoparticles had the best cellular uptake, whereas the 50nm nanoparticles had the smallest cellular uptake. The cellular uptake of polystyrene (PS) nanoparticles and poly(lactic-co-glycolic acid) (PLGA) nanoparticles coated with polyvinyl alcohol (PVA) or vitamin E TPGS was also measured. The Vitamin E TPGS-coated PLGA nanoparticles had better cellular uptake than the PS nanoparticles and the PVA-coated nanoparticles.[4] In another study, Verma and co-workers compared the cell-membrane penetration achieved by two nanoparticles that differed in the arrangement of surface hydrophilic and hydrophobic groups but had the same size, shape and ratio of hydrophobic to hydrophilic molecules.[5] One type of nanoparticle was coated with striations of alternating anionic and hydrophobic groups and the other type was coated with random distribution of anionic and hydrophobic groups. They found that the striated nanoparticles were able to pass directly through cell membranes and did not undergo endocytosis (a process by which material to be internalized is engulfed by a portion of the plasma membrane, which then buds off inside the cell to form a vesicle containing the ingested material[8]) or pinocytosis to reach the cytosol. In

contrast the nanoparticles with the random distribution of anionic and hydrophobic groups were almost completely blocked from cell entry.[5]

An alternative albeit indirect way to quantify cellular uptake of different types of nanoparticles is to measure the cytotoxicity that can accompany this process. For example, Pan and co-workers studied the cytotoxicity of gold nanoparticles with diameters ranging in size from 0.8nm to 15nm in four cell lines.[2] They also tested the toxicity of very small (diameter <0.8nm) gold particles (gold thiomalate). They found that nanoparticles with diameters in the size range from 1 – 2nm were more toxic to all four of the cell lines tested than the very small gold nanoparticles (gold thiomalte) or the larger 15nm particles. The authors speculate that the nanoparticle toxicity was a result of endocytosis, however, their experimental methods did not allow them to determine an exact cause of cell death.[2]

In addition to the experimental work that has been performed to examine nanoparticles and membranes, various approaches to modeling the interaction between nanoparticles and membranes with simulations have been described in the literature.[13, 14] The levels of detail used to represent the molecules in these models fall roughly in two main categories: high-resolution and low-resolution. High-resolution or atomistic models represent the geometry and energetics of all molecules realistically and typically account for the motion of every atom including every solvent atom. Atomistic simulations were used by Bedrov and co-workers to investigate the interaction and passive transport of C_{60} fullerenes into lipid membranes composed of di-myristoyl-phosphatidylcholine (DMPC).[15] The

system contained a DMPC bilayer composed of 52 lipid molecules and 1800 water molecules. The Lucretius molecular dynamics simulation package [15] was used along with the lipid force field parameters from CHARMM27.[16] The free energy and the diffusivity of the fullerene were obtained as a function of its position within the membrane; these properties were used to calculate the membrane permeability.[15]

Coarse-grained models of lipid and nanoparticle systems are low-resolution models that are based on a simplified representation of molecular geometry and energetics. In a coarse-grained model a single interaction site is used to represent a group of several atoms. This reduces the total number of sites whose trajectories must be calculated, thereby increasing the speed of the simulation. One example of a low-resolution model used to describe nanoparticle membrane interactions is that developed by Vacha and coworkers to study the passive endocytosis of ligand-coated nanoparticles of different sizes, shapes, coverage and membrane-binding strength.[17] For this work the authors used the implicit-solvent model for phospholipid membranes developed by Cooke et al.[18] In this model, three spheres are used to represent each phospholipid molecule: a hydrophilic sphere to represent the phospholipid headgroup and two hydrophobic spheres to represent the two phospholipid tails. The nanoparticles are composed of several spheres that are the same size as the hydrophilic headgroup sphere, most of which are hydrophilic. All simulations were performed using the ESPRESSO molecular dynamics package.[19] Vacha and coworkers demonstrated that larger spherical particles experienced endocytosis more easily than smaller particles. The authors

explain that this observation is a result of the more favorable compromise between bending rigidity and surface adhesive energy for the larger nanoparticles than for the smaller particles. The results also show that it is easier for spherocylindrical particles to undergo endocytosis than spherical particles. In addition, the authors demonstrate how endocytosis is suppressed for particles with sharp edges.[17]

An example of the use of a coarse-grained model to determine how a nanoparticle's size affects its translocation across a lipid bilayer is work by Lin and co-workers.[20] The nanoparticles in these explicit–solvent simulations were hydrophobic and ranged in size from 1.284 nm to 2.912 nm.; the lipid chosen for study was DPPC. All simulations were run using GROMACS 3.3.3 [21] with the MARTINI force field developed by Marrink et al.[22,23] Results showed that the time required for a nanoparticle to translocate to different positions in a DPPC bilayer (composed of 512 lipids) decreased with the size of the nanoparticle.[20] Yang and Ma also used coarse-grained computer simulations based on dissipative particle dynamics (DPD) to simulate the translocation of nanoparticles with different shapes across a lipid bilayer.[24] The lipid molecules, which contained two hydrophilic head spheres and five hydrophobic tail spheres, were constructed by arranging hydrophilic DPD spheres in the desired geometrical shape. The nanoparticles studied had a variety of geometries The simulations predicted the translocation of nanoparticles through the lipid membrane but not the endocytosis of the nanoparticles by the membrane. The authors concluded that the nanoparticle shape and initial orientation significantly affect the interaction between the nanoparticle and the lipid bilayer.

In this paper, we use an implicit-solvent intermediate-resolution model for lipid molecules, which we call "LIME," with discontinuous molecular dynamics (DMD), a fast alternative to traditional molecular dynamics simulation, to model the interaction between both hydrophilic and hydrophobic nanoparticles and DPPC bilayer membranes. The LIME geometric and energetic parameters for the DPPC lipids were obtained using a multiscale modeling approach as described in our previous paper.[6] In multiscale modeling atoms are grouped into coarse-grained sites and the geometric and energetic parameters for these coarse-grained sites are extracted from atomistic simulations in explicit solvent. The nanoparticle is modeled as a single sphere, essentially a generic nanoparticle, rather than as a cluster of spheres as other investigators have done. This is in keeping with our vision of this work as "proof of method" simulation, which could eventually evolve into examinations of more specific nanoparticle-membrane systems. Two types of nanoparticles are examined, hydrophilic and hydrophobic. The hydrophilic nanoparticles have square-well interactions with hydrophilic lipid sites and the hydrophobic nanoparticles have square-well interactions with hydrophobic lipid sites in our model. We investigate the extent to which hydrophilic nanoparticles with diameters from 5-100 Å are wrapped by a DPPC membrane and the extent to which hydrophobic nanoparticles with diameters from 5-20 Å penetrate the membrane. The largest hydrophobic nanoparticles that we chose to study had a diameter of 20 Å so that they could still fit within the hydrophobic portion of the DPPC bilayer. We also examine how the nanoparticle mass per volume affects the wrapping process.

Highlights of our results include the following. Our model demonstrates the major role that nanoparticle size plays in the membrane wrapping process. We find that hydrophilic nanoparticles with a diameter less than 20Å are not wrapped by bilayers; instead they become embedded in the bilayer's surface where they can interact with the hydrophilic head groups of the lipid molecules. Hydrophilic nanoparticles with diameters between 20Å and 100Å do undergo the wrapping process with the bilayer membrane. Hydrophobic nanoparticles with diameters of 5Å, 20Å and 40Å do not undergo the wrapping process; instead they directly penetrate the membrane and remain within the inner hydrophobic core of the bilayers. These findings are consistent with experimental results. Our results also showed that the rate of wrapping decreases with an increase in nanoparticle size for hydrophilic nanoparticles.

Methods and Model

To simulate the DPPC molecules in this work, LIME, an intermediate resolution implicit-solvent model for lipid molecules [6] developed for use with discontinuous molecular dynamics was employed. In LIME each DPPC molecule is represented by 14 coarse-grained sites and each coarse-grained site is classified as one of six unique coarse-grained types (I-VI). A detailed description of the coarse-grained parameters used to describe each DPPC molecule is provided in our previous work.[6] **Figure 2** illustrates the coarse-grained representation of: (a) a DPPC molecule and (b) a nanoparticle. Types I and II represent the choline entity and the phosphate group, respectively. Types III and IV are assigned to ester

coarse-grained sites 3 and 9, respectively. Type V is used to represent the coarse-grained sites in the hydrocarbon tails (excluding the terminal sites). Finally, type VI is used to classify the terminal tail coarse-grained sites. Each nanoparticle in our simulations is represented by one single coarse-grained site and is assigned the coarse-grained type VII.

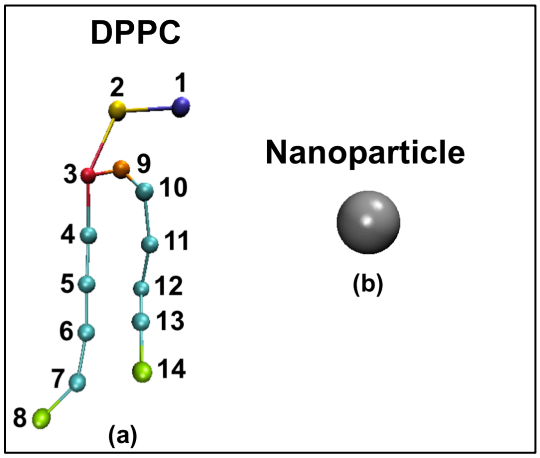

Figure 1: (a) Coarse-grained representation of DPPC (b) Coarse-grained representation of a nanoparticle. The color scheme is; purple (choline entity – type I for DPPC site 1); yellow (phosphate group – type II for DPPC site 2); red (ester group – type III for DPPC site 3); orange (ester group – type IV for DPPC site 9); cyan (alkyl tail groups – type V for DPPC sites 4-7&10-13); green (terminal tail groups – type VI for DPPC sites 8&14); gray (nanoparticle – type VII for nanoparticle site 1). The size of the DPPC coarse-grained sites and the nanoparticle are not drawn to scale.

The discontinuous molecular dynamics (DMD) algorithm, a very fast alternative to traditional molecular dynamics simulation, is the simulation method used for this work.[25,26] In DMD simulations, particles interact via a combination of hard-sphere and square well-potentials which means that the forces on particles need only be calculated when discontinuities in the potential are encountered. This allows for faster simulations than traditional molecular dynamics, enabling examination of larger systems and longer time scales. A hard sphere is an impenetrable, solid sphere; a square-well is a hard sphere surrounded by an attractive well. The square well (SW) potential between spheres *i* and *j* is given by:

$$u_{ij}^{SW}(r) = \begin{cases} \infty & r \le \sigma_{ij} \\ -\varepsilon_{ij} & \sigma_{ij} < r \le \sigma\lambda_{ij} \\ 0 & r > \lambda_{ij} \end{cases} \qquad \text{Equation 1}$$

where r is the distance between spheres, σ_{ij} is the hard sphere diameters, $\sigma\lambda_{ij}$ is the well diameter and ε_{ij} is the well depth. In our DMD simulations, the initial velocities assigned to coarse-grained sites are based on a Maxwell-Boltzmann distribution about the desired simulation temperature. The particle trajectories are then followed by calculating the time between each collision and advancing the simulation to the next event. Types of events include a collision between two hard spheres, a bond event when the distance between two bonded spheres reaches a minimum or maximum limit, and square well events when two spheres enter (capture), unsuccessfully attempt to escape (bounce) or successfully leave (dissociation) a square well.[25,26,27,28]

In all LIME/DMD simulations the simulation temperature is expressed in terms of the reduced temperature :

$$T^* = k_B T/\varepsilon^* \qquad \text{Equation 3}$$

where k_B is Boltzmann's constant, T is the temperature, and ε* is a reference interaction strength, which is the same as the reference interaction strength, ε* = 0.0363 that was used previously for our simulations of DPPC lipids at 325K.[29] Thus when $T^* = k_B T/\varepsilon^* = (8.6173 \times 10^{-5} \text{eV/K})*(325\text{K})/(0.363\text{eV}) = 0.77$ in our DMD/LIME simulations, the lipid molecules will behave as they would at a real temperature of 325K. A detailed description of the procedure used to calculate this value is provided in our previous work.[6]

The LIME σ_{ij}, $\sigma\lambda_{ij}$, and ε_{ij} coarse-grained parameters for DPPC molecules were obtained using a multiscale modeling technique. In this procedure coarse-grained parameters are extracted from data collected from atomistic simulations. Data used to calculate the DPPC parameters were obtained by running united-atom explicit-solvent simulations at T=325K of 30 DPPC lipids using the GROMACS simulation package [30,31] version 4.5.4 along with the GROMOS96 53a6 forcefield.[32] Complete details of the multiscale modeling procedure used to calculate the LIME DPPC parameters and the values of the σ_{ij}, $\sigma\lambda_{ij}$, and ε_{ij} parameters for DPPC molecules are provided in our previous publication.[6] In addition to extracting the σ_{ij}, $\sigma\lambda_{ij}$, and ε_{ij} coarse-grained parameters, the GROMACS simulation data was used to calculate the minimum and maximum bond and pseudobond lengths between coarse-grained sites. Pseudobonds are used in the model to maintain the relative

stiffness of the lipid molecules by limiting the fluctuation of the coarse-grained sites to the angles and torsional angles observed during the GROMACS simulation.

The coarse-grained interaction parameters between the nanoparticle and the DPPC sites were chosen to allow us to study the behavior of nanoparticles with diameters ranging in size from 5 – 100 Å. For this work we studied the interaction of the DPPC bilayer membrane with both hydrophilic and hydrophobic nanoparticles so that we could compare our results to data on nanoparticles with a wide range of hydrophobicities. We chose to model hydrophilic nanoparticles as spheres that interacted strongly with the hydrophilic lipid head groups of the DPPC molecules. (Since the hydrophilic lipid head groups in LIME have stronger interaction energies with each other than with the hydrophobic tail groups, we assumed that a hydrophilic nanoparticle would also have stronger interaction energies with the hydrophilic lipid head groups than with the hydrophobic tails.) To model these interactions the ε_{ij} values between DPPC coarse-grained sites 1 (choline entity), 2 (phosphate group) 3 (ester group) and 9 (ester group) and hydrophilic nanoparticles were each set to -2.0 eV, which is much larger than the average intermolecular ε_{ij} value of -0.036eV for DPPC coarse-grained sites. A value of -2.0 eV was chosen because it represents a very strong attraction (large well-depth) and we felt it would give us a good idea of the way that very hydrophilic nanoparticles would interact with a membrane. The ε_{ij} between the hydrophilic nanoparticles and all of the DPPC akyl tail groups (coarse-grained sites 4-8 and 10-14) were chosen to be zero, i.e. they interact as hard-spheres. The $\sigma\lambda_{ij}$ values between hydrophilic nanoparticles and DPPC coarse-grained sites 1 (choline entity), 2

(phosphate group) 3 (ester group) and 9 (ester group) were set to a value that made the width of the square-well interaction ($\sigma\lambda_{ij}$ - σ_{ij}) equal to 5.0 Å. Since this work was not performed to model any specific nanoparticle/bilayer system, we did not have any atomistic or experimental data to help us select the range for the square-well interactions between the nanoparticle and lipid head groups. We chose the range to be 5.0 Å **,** long enough for the lipids to feel the nanoparticles and want to wrap around them but not so long that the lipids could have square-well interactions with the nanoparticle without having to wrap around them. In addition, 5.0 Å is less than the 10.0 Å cutoff radius we use when we run atomistic simulations to obtain relatively realistic coarse-grained parameters for the lipid/nanoparticle interactions.

The interaction parameters between nanoparticle and lipid for the hydrophobic nanoparticle case were chosen in the following way. Since the hydrophobic lipid tails in LIME have much stronger interactions with each other than they do with the hydrophilic lipid head groups, we assumed that hydrophobic nanoparticles would prefer to interact with the hydrophobic lipid tails rather than with the hydrophilic lipid head groups. To model these interactions the hydrophobic nanoparticles were assigned square-well interactions of strength ε_{ij} = -2,0eV with the hydrophobic tails (coarse-grained sites 4-8 and 10-14) and hard-sphere interactions with the DPPC coarse-grained sites 1 (choline entity), 2 (phosphate group) 3 (ester group) and 9 (ester group). The $\sigma\lambda_{ij}$ value between hydrophobic nanoparticles and DPPC coarse-grained sites 4-8 and 10-14

(hydrophobic alkyl tails) was set to a value that made the width of the square-well interaction ($\sigma\lambda_{ij}$ - σ_{ij}) equal to 5.0 Å.

Each simulation was started from a preformed DPPC bilayer containing either 1500, 2500 or 4000 molecules. The bilayers composed of 1500, 2500 and 4000 lipids were built to span areas of 218Å x 218Å, 281Å x 281Å , 356Å x 356Å in the center of boxes with dimensions of 250Å x 250Å x 250Å. 400Å x 400Å x 400Å and 600Å x 600Å x 600Å, respectively. In all cases the bilayer was placed in a position where it could not interact with its periodic boundary image in each simulation. This was done to prevent the surface tension of the bilayer from affecting its interaction with the nanoparticle. Each nanoparticle was initially placed at the center of the bilayer, approximately 5Å above the preformed bilayer, far enough from the bilayer to prevent any overlaps, yet close enough to begin interacting with the bilayer. We chose to position nanoparticles close to the bilayers to avoid spending computational resources on simulations in which the nanoparticles did not interact with the bilayer. All simulations were run at a T* = 0.77.

Results and Discussion

DMD simulations were conducted to study the interaction between hydrophilic nanoparticles with a range of different physical properties and a bilayer composed of DPPC molecules. The nanoparticles in each simulation had diameters and densities ranging from 5–100 Å and 0.01–0.67 amu/Å^3, respectively, reflecting the fact that nanoparticles are made from a variety of materials. We decided not to study nanoparticle densities larger than 0.67 amu/Å^3 because this would have

significantly reduced the speed of our simulations. Increasing nanoparticle density decreases its velocity making it take longer to travel to the surface of the bilayer membrane. (Our goal was to model the nanoparticle/bilayer interaction and not the behavior of the nanoparticle before it reaches the membrane surface.) Note that the mass per volume of gold and silver nanoparticles is 116 and 6.3 amu/Å^3, respectively, much higher than the masses per volume we studied. The densities of the nanoparticles that we studied are more similar to the densities of silicon dioxide and polystyrene nanoparticles, which are approximately 1.4 amu/Å^3 and 0.63 amu/Å^3, respectively.[33,34] The lowest mass per volume that we studied , 0.013 amu/Å^3, was so low as to be unrealistic. We studied it anyway, because we felt it would allow us to determine whether or not density played a major role in the behavior of the nanoparticles in our model.

Simulations were conducted for ten different parameter sets; due to the computational intensity we only conducted a single run for each set. . **Table 5** lists the nanoparticle diameter, mass, and hydrophobicity and the number of DPPC lipids present in each simulation.

Run #	**Nanoparticle Diameter (Å)**	**Nanoparticle Mass Density (amu/Å^3)**	**Hydrophobicity**	**Number of DPPC lipids**
1	5	0.01	hydrophilic	1500
2	5	0.67	hydrophilic	1500

3	10	0.01	hydrophilic	1500
4	20	0.01	hydrophilic	1500
5	40	0.01	hydrophilic	1500
6	40	0.13	hydrophilic	1500
7	60	0.01	hydrophilic	2500
8	100	0.01	hydrophilic	4000
9	5	0.67	hydrophobic	1500
10	20	0.01	hydrophobic	1500
11	5	0.01	hydrophobic	1500
12	40	0.03	hydrophobic	1500

Table 5: The nanoparticle diameter, nanoparticle hydrophobicity, nanoparticle mass and number of DPPC lipids in each simulation.

Figures 2 (a) – (h) provide snapshots of runs 1 – 8 (described in **Table 5**), respectively, taken after 2500 million collisions in simulations of systems containing hydrophilic nanoparticles and lipid membranes. Each figure shows the interactions between the nanoparticle and the DPPC lipids. Comparison of the various panels makes it apparent that nanoparticle size plays a major role in determining whether or not a hydrophilic nanoparticle will be wrapped by a lipid bilayer. Hydrophilic nanoparticles with diameters of 5 Å and 10 Å (**Figure 2a – 2c)** embed themselves within the hydrophilic portion of the bilayers but do not get wrapped. Hydrophilic nanoparticles with diameters of 20, 40, 60 and 100 Å (**Figure 2d – 2h)** do get wrapped. Two simulations were run on the 5 Å hydrophilic nanoparticles to

determine how nanoparticle mass, 0.82amu or 43.6amu, affected the results. Interestingly the mass difference in the two nanoparticles did not change the outcome. In both of the simulations, the nanoparticles embedded themselves in the membrane next to the hydrophilic head groups of the lipids. Simulations were also run to compare the behavior of hydrophilic nanoparticles with a diameter of 40 Å and a mass of 420.0amu or 4200.0amu. The results of these simulations are shown in **Figure 2e** and **2f**, respectively. Again, there was no significant difference between the outcomes of the two simulations. We conclude that the nanoparticle mass per volume does not significantly affect the extent to which a hydrophilic nanoparticle is wrapped by a DPPC bilayer.

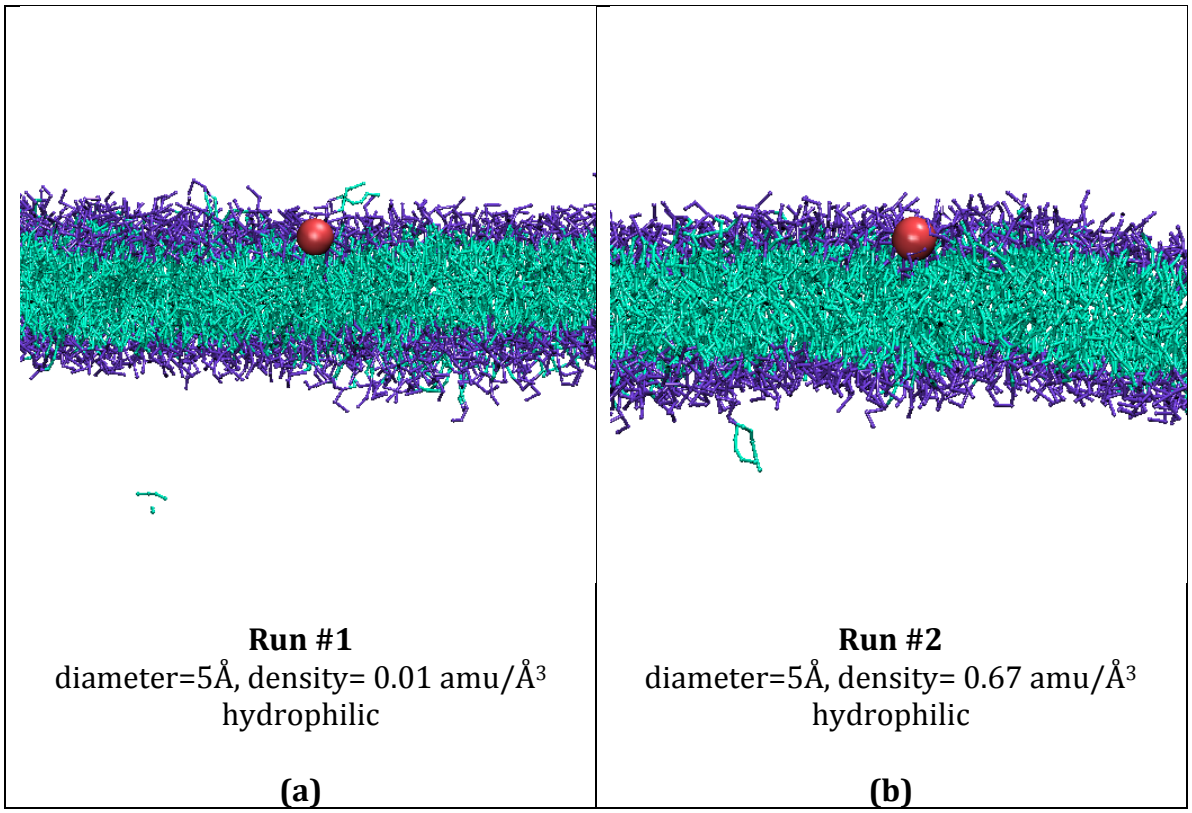

Run #1
diameter=5Å, density= 0.01 amu/Å^3
hydrophilic

(a)

Run #2
diameter=5Å, density= 0.67 amu/Å^3
hydrophilic

(b)

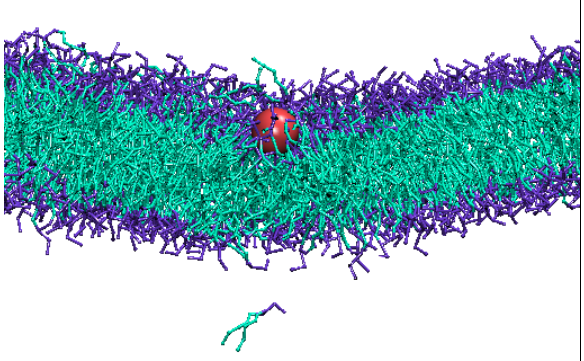

Run #3
diameter=10Å, density= 0.01 amu/Å^3
hydrophilic

(c)

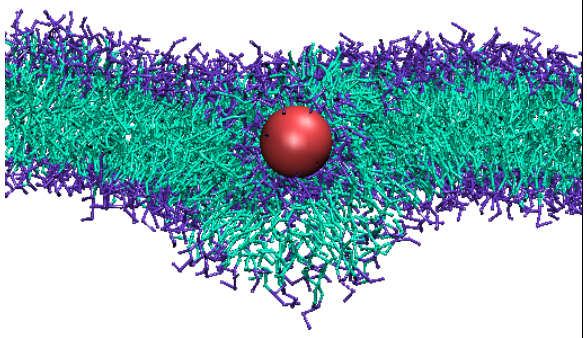

Run #4
diameter=20Å, density= 0.01 amu/Å^3
hydrophilic

(d)

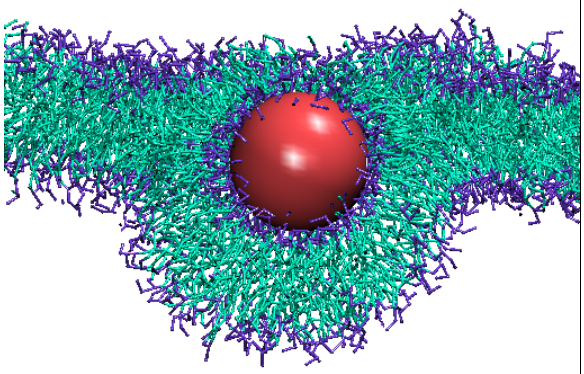

Run #5
diameter=40Å, density= 0.01 amu/Å^3
hydrophilic

(e)

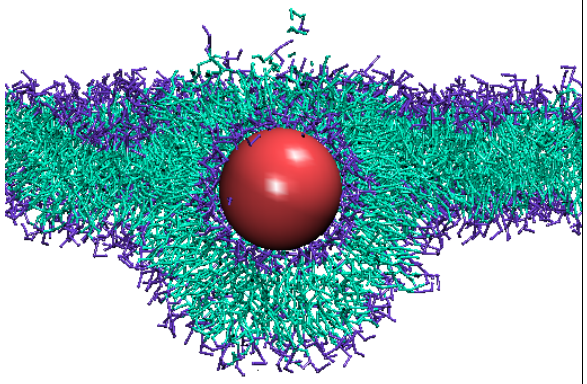

Run #6
diameter=40Å, density= 0.13 amu/Å^3
hydrophilic

(f)

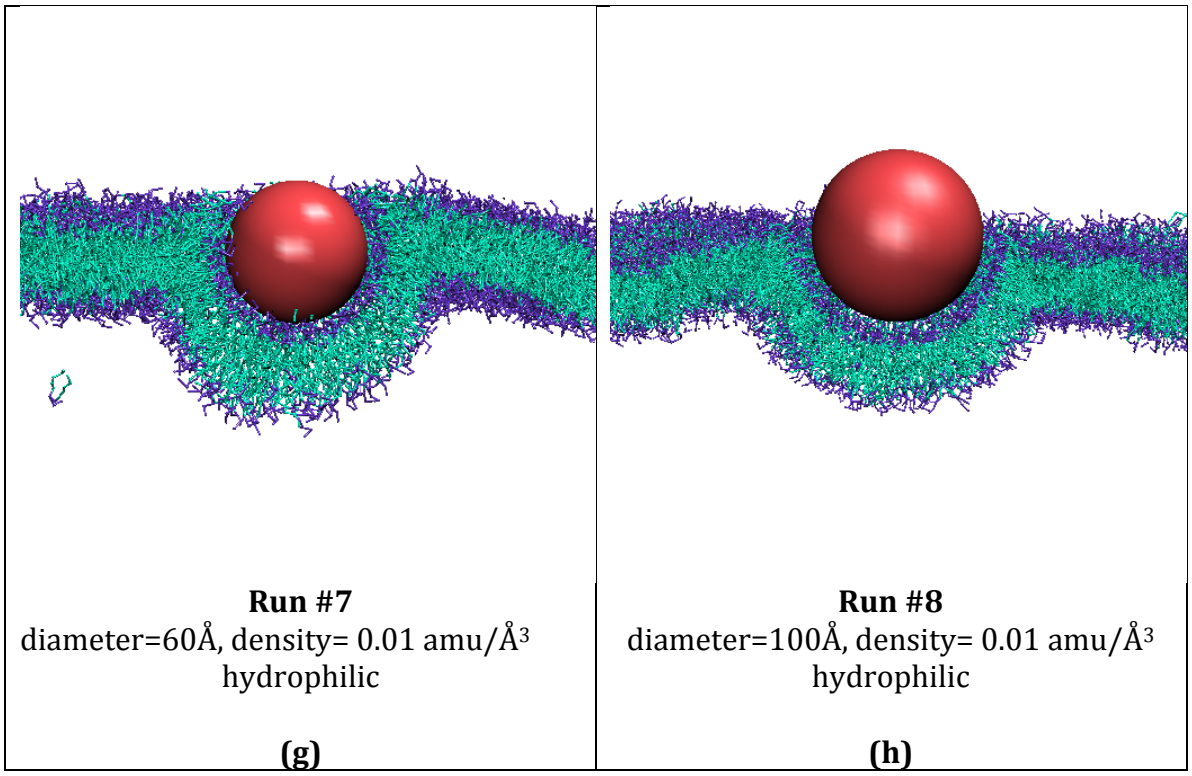

Figure 2: Snapshots of final configurations for simulations run on systems containing hydrophilic nanoparticles of different sizes and mass/volume and a DPPC bilayer membrane. Run 1 (a), 2 (b), 3 (c), 4 (d), 5 (e), 6 (f), 7 (g), 8 (h). The color scheme is: purple (DPPC choline entity), orange (DPPC phosphate group), red (DPPC ester groups), cyan (DPPC alkyl tail groups), red (nanoparticles).

Figure 3 shows the difference between the z position (the bilayer normal points in the z direction) of the DPPC headgroups (coarse-grained type 1) in square-well contact with the nanoparticle and the z position of the DPPC headgroups not in square well contact with the nanoparticle as a function of time for runs #2, #4 and #6. This gives us a measure of the degree of penetration/wrapping of the membrane by the nanoparticle as a function of time. Here by square well contact we mean coarse-grained sites interacting via a square-well potential with each other. We can see that as the nanoparticle becomes wrapped in runs #4 and #6 and moves down

through the bilayer, the average distance (in the z-direction) between DPPC headgroups in contact with the nanoparticle and not in contact with the nanoparticle increases. **Figure 3** also shows that for run #2, in which the nanoparticle does not become wrapped (it just stays within the hydrophilic portion of the membrane), the distance (in the z-direction) between DPPC headgroups in and out of square well contact with the nanoparticle fluctuates, but does not increase over time since the nanoparticle does move through the bilayer.

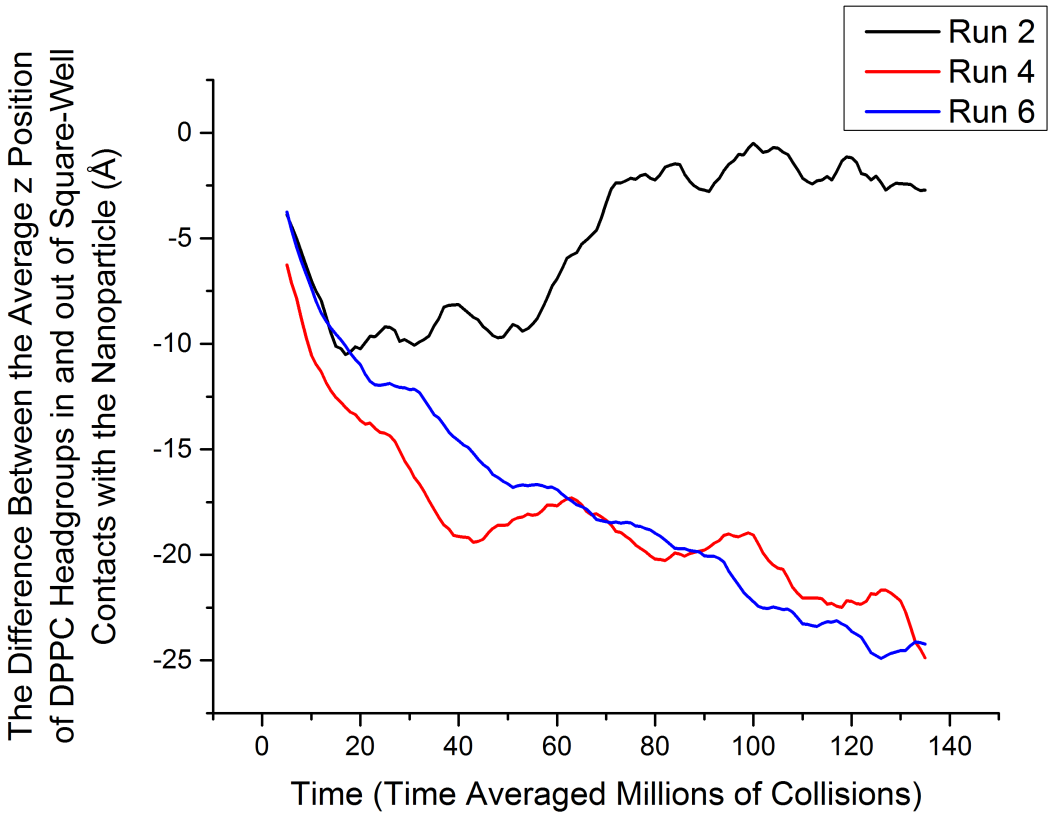

Figure 3: The difference between the average z position of DPPC headgroups in square-well contact and not in square well contact with the nanoparticle versus time for Runs #2, #4 and #6.

Figure 4 shows the fraction of a nanoparticle wrapped by DPPC lipids as a function of time for hydrophilic nanoparticles with diameters of 20Å (Run #4), 40Å (Run #5), 40Å (Run #6), 60Å (Run #7) and 100Å (Run #8). The nanoparticle mass densities were all 0.01 amu/Å^3 except for Run #6 which had a nanoparticle mass density 0.13 amu/Å^3. We see that the time required for complete wrapping decreases as nanoparticle size increases. Since the nanoparticle in Run #5 achieved approximately the same wrapping fraction as a function of time as the nanoparticle in Run #6 it appears that for equi-sized nanoparticles, mass density does not play a role in the rate of wrapping.

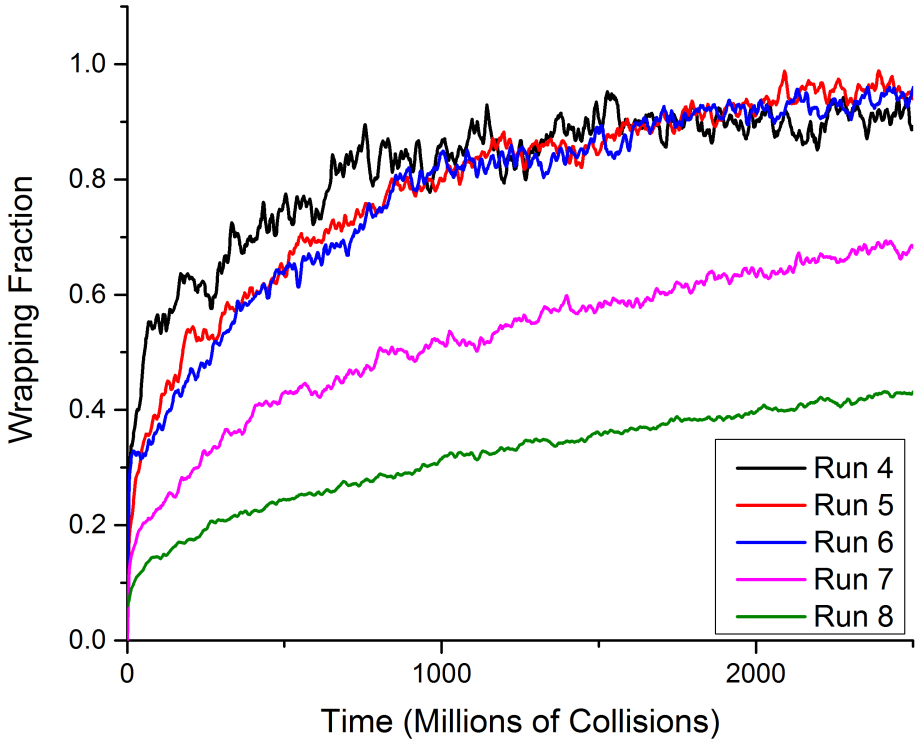

Figure 4: The wrapping fraction as a function of time for nanoparticles with diameters of 20Å (Run #4), 40Å (Run #5), 40Å (Run #6), 60Å (Run #7) and 100Å (Run #8). The nanoparticle mass densities were 0.01 amu/Å^3 for Run #4, #5, #7 and #8 0.13 amu/Å^3 for Run #6. The time is displayed as the time in millions of collisions.

Figure 5 provides snapshots at different time points during run #6, where a hydrophilic nanoparticle with a diameter of 40Å and mass density of 0.13 amu/Å^3 is wrapped by a bilayer. At 25 million collisions (**Figure 5a**) the nanoparticle reaches the surface of the membrane and is then slowly wrapped by the bilayer in **5b** (625 million collisions), **5c** (1250 million collisions) and **5d** (3000 million collisions). The

same wrapping process was observed for all other hydrophilic nanoparticles with a diameter greater than 20Å.

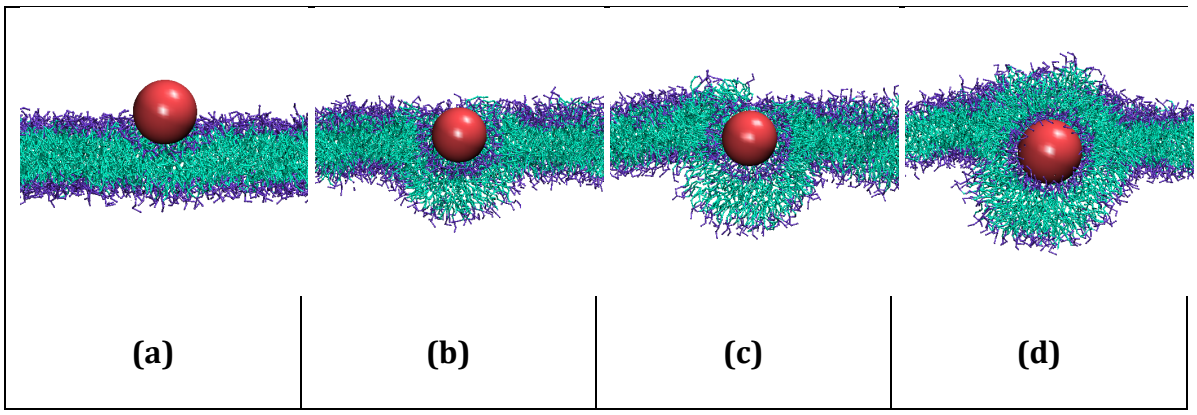

Figure 5: Snapshots from run #6 in which a hydrophilic nanoparticle with diameter 40Å is wrapped by a bilayer membrane composed of 1500 DPPC lipids. The nanoparticle (a) reaches the surface of the bilayer at 25 million collisions. The wrapping process continues at (b) 625 million collisions, (c) 1250 million collisions and (d) 3000 million collisions.

Figure 6 provides simulation snapshots of the embedding of a hydrophobic nanoparticle with a diameter of 20 Å by DPPC bilayers at three different time points in run #10. **Figure 6a** shows the hydrophobic nanoparticle approaching the surface of the membrane after 25 million collisions. By 50 million collisions , **Figure 6b,** the nanoparticle has entered the lipid bilayer but continues to interact with both the hydrophilic head groups and hydrophobic tails of the DPPC lipids. **Figure 6c** shows the nanoparticle after it has completely embedded itself within the inner hydrophobic core of the membrane at 225 million collisions. In fact, the nanoparticle completely embeds itself within the membrane by 75 million

collisions; there is no visible change in the configuration between the 75 million and 225 million collisions. Since this simulation ran at a rate of approximately 4 million collisions per hour, the time required for the nanoparticle to completely embed itself within the bilayer membrane is approximately 19 CPU hours.

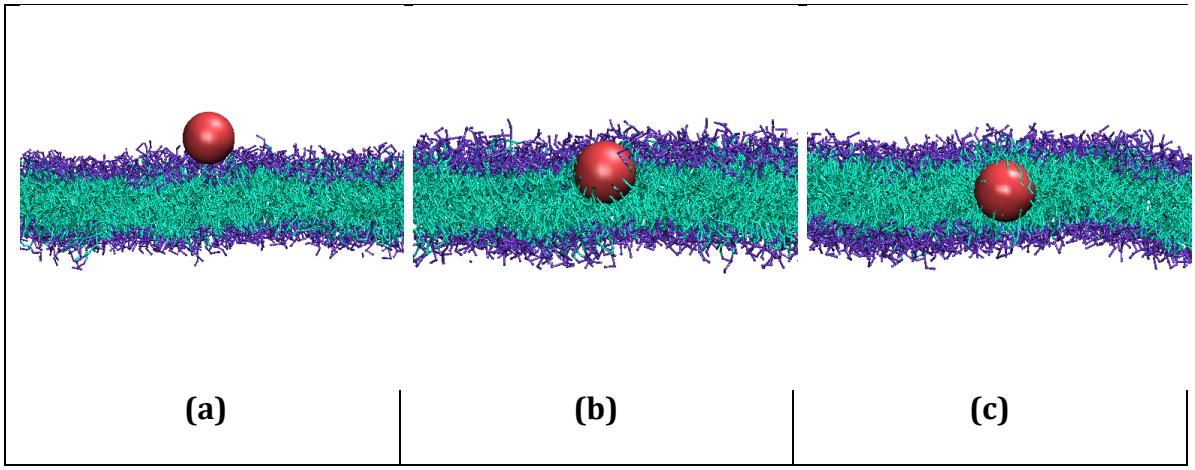

Figure 6: Snapshots from run #10 in which a hydrophobic nanoparticle with a diameter of 20Å embeds itself in a DPPC bilayer composed of 1500 lipids. The nanoparticle (a) reaches the surface of the bilayer after 25 million collisions, (b) begins to penetrate the membrane after 50 million collisions, and (c) is fully embedded within the inner hydrophobic core of the membrane after 225 million collisions.

Simulation results showing the interaction between hydrophobic nanoparticles and bilayer membranes from runs #9, #11 and #12 with nanoparticle diameters/mass densities of 5Å/ 0.67amu/Å^3, 5Å/ 0.01 amu/Å^3 and 40Å/ 0.03 amu/Å^3 were very similar to those of run #10 (20 Å/ 0.01 amu/Å^3) . Therefore, we conclude that for hydrophobic nanoparticles within this size range, size does not affect the way in which the nanoparticle penetrates the membrane or embeds itself within the

hydrophobic core of the bilayer. In runs #9 and #11 we simulated the behavior of nanoparticles with the same diameter but with different masses (43.6 amu and 0.82 amu) respectively. Again, we did not see a difference in the movement of the nanoparticles through the hydrophilic headgroups to the hydrophobic portion of the membrane , indicating that the mass per volume of the nanoparticles did not affect their interaction with the bilayer membrane.

Figure 7 shows the time averaged distance from the nanoparticle to the plane through the center of the bilayer for runs #9, #10, #11 and #12. The plane that goes through the center of the bilayer was calculated as the average z-position of the terminal tail coarse-grained sites of all DPPC lipids on both layers not in a square-well interaction with the nanoparticle. This plane fluctuated by a small amount over the course of each simulation; however, the location of the plane was recalculated for each time point included in **Figure 7**. **Figure 7** also shows that for runs #9, #10, #11 and #12 (hydrophobic nanoparticles with diameters of 5Å, 20Å, 5Å and 40Å, respectively) once the nanoparticle starts to experience square-well interactions with the bilayer, the distance between the nanoparticle and the plane through the bilayer center decreases as a function of time until it reaches approximately 0 Å. Once each hydrophobic nanoparticle reaches the plane through the bilayer center, the distance between the nanoparticle and the bilayer fluctuates slightly but overall remains almost constant. It can be seen that the 5Å nanoparticle in runs #9 and #11 reaches the plane through the bilayer center faster than the 20Å nanoparticle in run #10, which is itself faster than the 40Å nanoparticle in run#12. Thus we see that the smaller the nanoparticle the faster it penetrates the bilayer to

reach the plane through the bilayer center. This makes sense, smaller nanoparticles have to push less lipids out of the way to penetrate the bilayer.

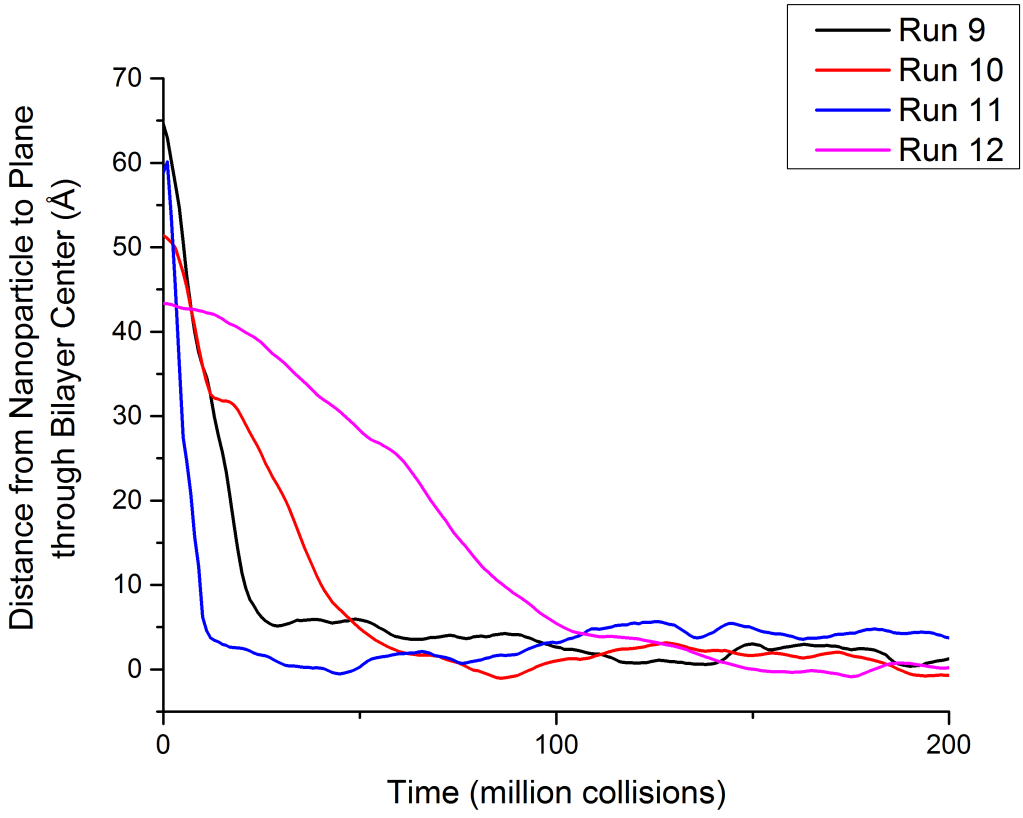

Figure 7: The distance from the nanoparticle to the plane through the bilayer center for runs #9, #10 #11 and #12. The zero time point for each run is set to the time when the nanoparticle first has a square-well interaction with a lipid tail coarse-grained site.

Conclusion

We describe the results of computer simulations performed to study the interaction between nanoparticles with a wide range of physical properties (sizes,

densities and hydrophobicities) with DPPC lipid membranes. Our model is generic, meant to give insights into the general biophysics associated with nanoparticle-membrane interactions. For this reason, we cannot compare our findings to any specific nanoparticle/membrane system because the parameters that we used for the nanoparticle in this model were not based on experimental work or on atomistic simulation.

Although not physically realistic, in this work we have decoupled particle volume from interaction strength. We selected a reasonable square-well width on the order of 5 Å, and interaction energies of -2.0eV for interactions between hydrophilic nanoparticles and hydrophilic lipid molecules and for interactions between hydrophobic nanoparticles and hydrophobic lipid molecules. In the future, we will utilize our multiscale modeling approach to obtain realistic square-well depths and widths for nanoparticles in the size range we found to be important from this work.

We chose to study both hydrophilic and hydrophobic nanoparticles to investigate the interaction between bilayer membranes and nanoparticles with different hydrophobicities. We successfully demonstrated that LIME/DMD can be used to model the process by which hydrophilic nanoparticles are either wrapped by a bilayer membrane or implant themselves on the surface of the membrane. We also show how hydrophobic nanoparticles spontaneously penetrate the lipid bilayer to embed themselves within the membrane core.

It is of interest to compare the trends that we have observed with those found in nature. Nanoparticle size is known to play a role in cellular uptake.

According to Nel and co-workers a threshold radius exists below which particles are incapable of entry and hence cellular uptake is reduced.[1] In addition, nanoparticles are thought to have optimal sizes which help to accelerate the wrapping process.[1,3,35] Values for the threshold radius and the optimal wrapping radius vary depending on nanoparticle properties. Our LIME/DMD simulations are consistent with this concept in that our model membrane would not wrap nanoparticles with a diameter below a critical value.

Our result that hydrophilic nanoparticles with a diameter less than 20Å get embedded as opposed to wrapped by the lipid bilayers is in agreement with the experimental observation of Bihan and co-workers. They showed that hydrophilic silica nanoparticles with diameters of approximately 15-20nm remained bound to the outer surface of a liposomal membrane and that hydrophilic silica nanoparticles with diameters of 30nm and 65nm were engulfed.[7] Note that we cannot directly compare our results to those of Bihan and co-workers because we did not simulate the behavior of the same type of nanoparticle.

We measured the wrapping fraction as a function of time for nanoparticles with diameters from 20Å - 100Å and found that the rate of wrapping decreases as nanoparticle diameter increases. These results were consistent with those of Gao and co-workers who observed a higher wrapping rate for small nanoparticles than for large nanoparticles during molecular dynamics simulations using the dissipative particle dynamics method.[36] In addition, we found that for nanoparticles of the same diameter, the mass density did not affect the rate at which the nanoparticle became wrapped by the membrane. We also studied the behavior of nanoparticles

with different mass per volume ratios (0.013 – 0.67 amu/Å^3). According to our investigations, aside from the rate of wrapping, the density of nanoparticles with the same volume did not affect their interaction with the bilayer membrane. In the future, we plan to simulate the behavior of specific nanoparticle/membrane systems with realistic estimates for the nanoparticle size, density and hydrophilicity .

We also studied the interaction between hydrophobic nanoparticles and the bilayer membrane. According to our simulations, hydrophobic nanoparticles embed themselves within the hydrophobic core of the bilayer membrane without becoming wrapped. This result is in good agreement with those of Li and co-workers who showed that in simulations of hydrophobic nanoparticles and DPPC bilayers the nanoparticle embeds itself into the hydrophobic core of the membrane.[9] Our results are also consistent with simulations performed by Qiao and co-workers who found that a hydrophobic fullerene C_{60} molecule easily embeds itself within a DPPC bilayer.[10] The authors explain that the adsorption of the C_{60} into the DPPC bilayer is driven by the interactions between the C_{60} and the lipid tails. In addition, the authors report that $C_{60}(OH)_{20}$ adsorbed onto the membrane instead of embedding within the bilayers because this functionalization of the fullerene made it hydrophilic.[11] In other experimentally-based studies, silver hydrophobic nanoparticles have been found to embed themselves inside the bilayer membrane regardless of the values for the mass per volume.[11,12] This was also the case in our simulations for both hydrophilic and hydrophobic nanoparticles with a mass per volume density within 0.12 – 0.67 amu/Å^3.

Since this work was essentially a proof-of-method study to see if LIME/DMD simulations were capable of mimicking the adsorption of a nanoparticle by a lipid membrane, we designed our systems to minimize simulation time, which is why we limited the diameter of our nanoparticles to the size range of 5Å - 100Å. We chose not to study nanoparticles larger than 100 Å because this would require extremely large bilayers to provide enough lipid molecules to fully wrap the nanoparticles, which would in turn require significant computational resources and time. In the future we would like to simulate systems with much larger nanoparticles (10nm – 100nm). Now that we have verified the ability of our model to properly simulate nanoparticle behavior, we are ready to invest the time required to model these larger systems.

One advantage that our LIME/DMD model has over other coarse-grained models reported in the literature is its speed. We demonstrated in our previous publication that LIME allows for the simulation of lipids at the fastest rate reported in the literature.[6] The is important for bilayer/nanoparticle studies because the number of molecules in bilayer/nanoparticle systems is often very large, requiring a very fast algorithm in order to simulate their behavior over desirable time scales. While the LIME/DMD model has many advantages for simulating the interaction between nanoparticles and lipid membranes it does have some disadvantages. Some of these limitations include: (1) electrostatics is not represented explicitly, (2) the use of an implicit solvent approach means that diffusion and hydrodynamics are not well represented, and (3) a direct correlation between reduced temperature and

real temperature can only be made at the temperature at which LIME was parameterized.

ACKNOWLEGEMENT

This work was supported by the National Institutes of Health under grants GM56766 and EB006006, and by the National Science Foundation under grant DMR-1206943. This work was also supported in part by NSF's Research Triangle MRSEC (DMR-1121107). EMC received a GAANN (North Carolina State University Graduate Assistance in Areas of National Need) Computational fellowship and a NIH/North Carolina State University Molecular Biotechnology Training Program fellowship. This work used the Extreme Science and Engineering Discovery Environment (XSEDE), which is supported by National Science Foundation grant number ACI-1053573. EMC received a startup research allocation from XSEDE, which helped complete the work described in this paper. We thank the National Institute for Computational Science (NICS), Texas Advanced Computing Center (TACC) and San Diego Supercomputer Center (SDSC) for providing us computing time. We also thank the Deutsche Forschungsgemeinschaft (DFG) for financial support via the International Research Training Group 1524 "Self-Assembled Soft Matter Nano- Structures at Interfaces

References

1. A. Nel, L. Madler, D, Velegol, T. Xia, E. Hoek, P. Somasundaran, F. Klaessig, V. Castranova, M. Thompson, *Nat. Mater.*, 2009, **8**, 543 – 557.

2. Y. Pan, S. Neuss, A. Leifert, M. Fischler, F. Wen, U. Simon, G. Schmid, W. Brandau, W. Jahnen-Dechent, *Small*, 2007, **11**, 1941 – 1949.
3. B. Chithrani, A. Chazani, W. Chan, *Nano Lett.*, 2006, **6**, 662 – 668.
4. K. Win, S. Feng, *Biomaterials*, 2005, **26**, 2713 – 2722.
5. A. Verma, O. Uzun, Y. Hu, Y. Hu, H. Han, N. Watson, S. Chen, D. Irvine, F. Stellacci, *Nature Mater.*, 2008, **7**, 588 – 595.
6. E. Curtis, C. Hall, *J. Phys. Chem. B.*, 2013, **117**, 5019-5030.
7. O.L. Bihan, P. Bonnafous, L. Marak, T. Bickel, S. Trepout, S. Mornet, F. De Haas, H. Talbot, J. Taveau, O. Lambert, *J. Struct. Biol.*, 2009, **168**, 419 – 425.
8. G.M. Cooper, *The Cell,* Sinauer Associates, Sunderland, 2nd edn., 2000.
9. Y, Li, X. Chen, N. Gu, *J. Phys. Chem. B*, 2008, **112**, 16647-16653.
10. R. Qiao, A.P. Roberts, A.S. Mount, S.J. Klaine, P.C. Ke, *Nano Lett.*, 2007, **7**, 614 – 619.
11. S. Park, S. Oh, J. Mun, S. Han, *Colloids Surf., B*, 2005, **44**, 117-122.
12. G. Bothun, *J. of Nanobiotechnol.*, 2008, **6**, 1-10.
13. A. H. Bahrami, M. Raatz, J. Agudo-Canalejo, R. Michel, E. Curtis, C. K. Hall, M. Gradzielski, R. Lipowsky, T. R. Weikl, *Adv. Colloid Interface Sci.*, 2014, **208**, 214-224.
14. H. Pera, T.M. Nolte, F.A.M. Leermakers, J. M. Kleijn, *Langmuir*, 2014, **30**, 14581 – 14590.
15. D. Bedrov, G. Smith, H. Davande, L. Li, *J. Phys. Chem. B.*, 2008, **112**, 2078 – 2084.
16. N. Foloppe, A. D. Jr. MacKerell, *J. Comput. Chem.*, 2000, **21**, 86 – 104.

17. R. Vacha, F. Martinez-Veracoechea, D. Frankel, *Nano Lett.*, 2011, **11**, 5391 – 5395.

18. I. R. Cooke, M. Deserno, *J. Chem. Phys.* 2005, **123**, 224710.

19. H. Limbach, A. Arnold, B. Mann, C. Holm, *Comput. Phys. Commun.*, 2006, **174**, 704 – 727.

20. X. Lin, Y. Li, N. Gu, *J. Comput. Theor. Nanosci.*, 2010, **7**, 269 – 276.

21. E. Lindahl, B. Hess, D. Van der Spoel, *J. Mol. Model*., 2001, **7**, 306 – 317.

22. S. Marrink, A. de Vries, A. Mark, *J. Phys. Chem. B.*, 2004, **108**, 750 – 760.

23. S. Marrink, H. Risselada, S. Yefimov, D. Tieleman, A. de Vries, *J. Phys. Chem. B.*, 2007, **111**, 7812 – 7824.

24. K. Yang, Y. Ma, *Nat. Nanotechnol.*, 2010, **5**, 579 – 583.

25. S. W. Smith, C. K. Hall, B.D. Freeman, *J. Comput. Phys.*, 1997, **134**, 26-30.

26. B. Alder, T. Wainwright, *J. Chem. Phys.*, 1959, **31**, 459 – 466.

27. DC. Rapaport, *J. Phys. A.*: *Math. Gen.*, 1978, **11**, L213 – L217.

28. DC. Rapaport, *J. Chem. Phys.*, 1979, **71**, 3299 – 3303.

29. H. D. Nguyen, C. K. Hall, *Proc. Natl. Acad. Sci. U.S.A.*, 2004, **101**, 16180 – 16185.

30. R. Faller, A. Marrink, *Langmuir*, 2004, **20**, 7686-7693.

31. D. Van der Spoel, E. Lindahl, B. Hess, G. Groenhof, A. Mark, H. Berendsen, *J. Computational Chemistry*, 2005, **26**, 1701 – 1719.

32. C. Oostenbring, A. Villa, A. Mark, W. Van Gunsteren, *J. Comput. Chem.*, 2004, **25**, 1656 – 1675.

33. US Research Nanomaterials, Inc. http://www.us-nano.com/inc/sdetail/408 (accessed April 2015)

34. G. Mahler, M. Esch, E. Tako, T. Southard, S. Archer, R. Glahn, M. Shuler, *Nat. Nanotechnol.*, 2012, **7**, 264 – 271.

35. P. Decuzzi, M. Ferrari, *Biomaterials*, 2007, **28**, 2915 – 2922.

36. X. Gao, J. Dong, X. Zhang, *Mol. Simul.*, 2014, **41**, 531-537.